Journal of Catalysis **201,** 80–88 (2001)
doi:10.1006/jcat.2001.3226, available online at http://www.idealibrary.com on IDEAL®

Reaction of HY Zeolite with Molecular Fluorine

Norma A. Sánchez,* José M. Saniger,*,[1] Jean-Baptiste d'Espinose de la Caillerie,† Alexander L. Blumenfeld,‡ and José J. Fripiat‡

*Laboratorio de Materiales y Sensores, Centro de Instrumentos, UNAM, Circuito exterior Cd. Universitaria, AP 70-186, CP 04510, México, D.F. Mexico; †Laboratoire de Physique Quantique, ESA CNRS 7069, ESPCI, 10 rue Vauquelin, 75231, Paris, Cedex 05, France; and ‡Department of Chemistry, University of Idaho, Moscow, Idaho 83844

Received November 30, 2000; revised March 10, 2001; accepted March 10, 2001; published online May 31, 2001

At room temperature, gaseous F_2 extracts tetrahedrally coordinated aluminum from the lattice of an acid, near-faujasite HY zeolite (Si/Al ≈ 13) and forms fluoro-hydroxy-aluminum complexes of the type $Al_2F(OH)_n^{(5-n)+}$ in which Al is octahedrally coordinated. Moreover, the crystallinity of the zeolite is almost unchanged by the fluorination process. The HY dehydrated at 200°C under vacuum and treated under a F_2 pressure of 300 mbar at room temperature is practically totally dealuminated. At lower pressure the transformation is partial. The coordination shell of the complex becomes unstable at about 500°C. Upon losing ligands, octahedral Al reverts partially to the tetrahedral coordination and is partially reinserted into the lattice. At a higher temperature an amorphous alumina phase is formed. ^{27}Al and ^{19}F high-resolution solid-state NMR, FT-IR, X-ray diffraction, and temperature-programmed desorption (TPD) are the main tools used in this work.

Key Words: **zeolite; dealumination; fluorination; ^{27}Al and ^{19}F NMR.**

INTRODUCTION

Fluorination modifies the catalytic properties of oxides. Formation of Al–F groups increases the Brønsted acid strength, which, otherwise, is negligible in alumina. Fluorination can also promote hydrogenation by alumina-supported sulfides (1). Generally speaking, the promotion effect of fluorine is not fully understood. On cracking catalysts, it might be rationalized in terms of its strong electron-withdrawing properties (2). Its promoting effect on hydrogenation could find its origin in an increased electronic density at the active sulfide site (3). However, in order to explain the occurrence of an optimum fluorine content, a precise identification of the fluorine sites is necessary. Recently, the surface structure of partially fluorinated aluminas has been described in terms of $Al^{VI}(O_{6-n}F_n)$ surface species. Based on IR or NMR results (4, 5) the existence of an $AlF_3 \cdot 3H_2O$ surface phase was postulated.

Both the Lewis and Brønsted acid sites of zeolites are deeply modified by fluorination. Panov *et al.* (6) have discussed the effect of fluorination by ammonium fluoride on the distribution of acid sites in ultrastable Y zeolite (USY). They have also summarized the literature on the influence of the fluorination on the catalytic properties of zeolites. There, the main effect of fluorination is to remove aluminum from the framework, thereby increasing the strength of the remaining framework Brønsted sites but decreasing the total amount of framework Brønsted and nonframework Lewis acid sites.

Here we will report on the effect of molecular F_2 on the structure of the acid near-faujasite HY zeolite. Due to environmental concerns, F_2 is not a classical fluorination agent. It presents, however, several advantages over NH_4F since it does not require calcination in order to incorporate fluorine, this last step producing by itself a noticeable dealumination of HY (7). Heating HY above 300°C also provokes dealumination (8) and it was observed that the NFAl particles remain in the microporous volume of the zeolite (9) in a way comparable to what has been shown in treating USY by NH_4 F and in calcining (6).

In order to study the influence of fluorination on the distribution of aluminum among the framework (FAl) and nonframework (NFAl) sites, ^{19}F and ^{27}Al high-resolution solid-state NMR spectroscopy was used extensively. In addition, FT-IR analyses of the volatiles evolving from the modified solid at high temperature were performed.

Earlier data by Lok *et al.* (10) have shown that the structure of the silicate backbone is not deeply affected by fluorination as indicated by the XRD, but the exact nature of the fluorinated nonframework aluminum species (Fl-NFAl), likely to affect the catalytic activity, remains to be uncovered. This is the purpose of this work. We will show that a fluorinated nonframework mobile species of compositions such as $Al_2F(OH)_n(H_2O)_m^{(5-n)+}$, where the aluminum is octahedrally coordinated, results from the reaction of HY with gaseous fluorine without the requirement of thermal activation.

[1] To whom correspondence should be addressed.

0021-9517/01 $35.00

EXPERIMENTAL

Sample preparation. The HY zeolite (CBV720, Zeolyst International) was outgassed at 200°C in the presence of a liquid nitrogen trap for at least 2 h in order to remove most of the physisorbed water and to minimize the formation of HF produced by reacting F_2 with H_2O. As stated above, a higher temperature would provoke dealumination (8). This pretreatment is a compromise: it lowers the intensity of the IR-active bending mode of water at $\approx$1630 cm^{-1} to a large extent while keeping the degree of dealumination as low as possible.

After outgassing, the temperature was lowered to 25°C, and dry F_2 (Air Products) in the presence of a NaF trap to remove HF contaminant was introduced for 10 min under pressures between 20 and 300 Torr. After 10 min no pressure change was noticeable, and F_2 was removed by pumping. The sample was kept in air until it was analyzed. From the initial HY, three samples (labeled F20, F100, and F300) were prepared using initial pressures of 20 Torr, 100 Torr, and 300 Torr, respectively. From F300, two additional samples were prepared: (i) F300H was obtained by heating in a He flow at 500°C for 1 h and (ii) F300C was obtained by calcining F300H at 1000°C for 10 min.

Temperature-programmed desorption (TPD) test. About 50 mg of fluorinated zeolite powders were initially dried at 500°C in a He flow, and then saturated at room temperature with ammonia in a 10% NH_3–He mixture, and finally calcined at 1000°C in a He flow.

All the thermal and absorption/desorption treatments were carried out *in situ* without exposing the sample to the atmosphere. The exhaust gases were measured with a thermal conductivity detector. The detector, valves, and tubing were kept at 160, 140, and 140°C, respectively, during the analysis.

MAS NMR ^{27}Al and ^{19}F. ^{27}Al NMR one-pulse spectra were obtained at a frequency of 130.3 MHz by spinning at 11.5 kHz and with a small tip angle of less than $\pi/12$ in order to permit quantification of Al contents (nonvisible Al contents were minimized). The pulse duration was 1 μs, and the recycle time was 1 s. A thousand scans were accumulated. The chemical shift reference was aqueous Al^{3+}.

^{19}F NMR one-pulse spectra at a frequency of 282.4 MHz were recorded by spinning at 17.5 kHz. The $\pi/2$ pulse duration was 2 μs, and the recycle time was 60 s. The chemical shifts were referred to C_2F_6 (−163 ppm CF_3Cl).

Chemical analyses. The SiO_2 and Al_2O_3 contents were obtained by X-ray fluorescence (11). The fluorine analyses were carried out by the potentiometric technique proposed by Bodkin (12). The sample was melted with lithium tetraborate and metaborate. It was then dissolved in nitric acid (10 wt%), and the EMF of the solution was compared to those obtained from standard solutions of NaF in the same solvent. The standard error on F determination was 10%.

FT-IR. The zeolite powder was spread over KBr windows for the observation of the lattice vibrations. The nature of the volatile removed from the solid in the course of the temperature-programmed desorption (TPD) was detected in an interface Nicolet TGA/FT-IR gas cell in a flow of argon.

XRD. The X-ray diffractograms were obtained on a Siemens D500 apparatus, using Cu $K\alpha 1$ radiation, an operating voltage of 30 kV, an electron current of 20 mA, and a scanning speed of 2° 2θ/min.

RESULTS AND DISCUSSION

Table 1 gives the chemical compositions, either in percent or in atoms per gram of dry zeolite. The correction factor was calculated from the sum of all analyzed elements and the difference from 100 was assigned to physisorbed water. The fluorine contents increase steadily as the F_2 pressure increases. They are in the range of those published earlier: in agreement with Panov *et al.* (6), the chemical ratio Si/Al is unaffected by the fluorination treatment. Here it was on average 12.7, instead of 15 according to the manufacturer.

The room temperature fluorination treatment affects deeply the Al distribution (Fig. 1). Besides the four-fold coordinated Al^{IV}, exclusively present in the original lattice (line at 63 ppm), an Al^{VI} resonance appears at −10 ppm. This shift is too negative to be assigned to an aluminum hexacoordinated to oxygen. Therefore, it must be attributed to a fluorinated species: it will be called Fl-NFAl. The intensity of the 63 ppm FAl resonance decreases with the F content while that of the −10 ppm resonance in Fl-NFAl increases. In F300, the residual intensity of the Al^{IV} is at the most 5% of the initial one in HY.

From the intensities of the ^{27}Al NMR resonances, the FAl/(initial FAl) ratio and the absolute lattice Al contents can be calculated from the chemical analyses, if it is assumed that there is no NFAl in HY. As shown in Fig. 1, the intensity of the line at about 2 ppm, due to Al^{VI} in NFAl in the original untreated sample, is small but not zero. Neglecting this small initial content means that the difference between

TABLE 1

Chemical Analyses

Sample	SiO_2 %	Al_2O_3 %	*F*, %	Corr	at Si/gZ $\times 10^{20}$	at Al/gZ $\times 10^{20}$	at F/gZ $\times 10^{20}$	Si/Al
HY	78.9	5.3	0	1.18	93.5	7.5	0	12.5
F20			0.044		93.6	7.3	0.14	
F100			0.524		93.6	7.4	1.66	
F300	84.7	5.7	1.27	1.10	93.6	7.4	4.03	12.7
F300H	86.2	5.7	0.966	1.08	93.7	7.3	3.06	12.8
F300C	92.2	6.2	0.264	1.01	93.6	7.4	0.84	12.7

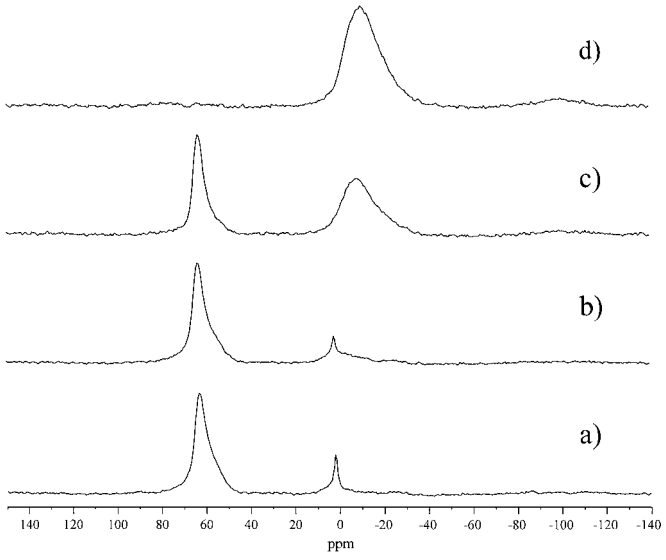

FIG. 1. ^{27}Al NMR spectra of (a) the starting HY material, (b) F20, (c) F100, and (d) F300 samples.

TABLE 2

Unit Cell Dimension *a* and Lattice Composition[a]

Sample	Average *a*, Å[b]	Avedev, Å[c]	% Relative crystallinity[d]	FAl/Si
Blank	24.2764	0.002477	100	12.64
F20	24.2759	0.003231	102	14.86
F100	24.251	0.00355	104	20.37
F300	24.21	0.01486	109	253.2
F300H	24.2173	0.007393	109	85.5
HY400	24.58	n.a.	~100	2.95
HY500	24.54	n.a.	~100	3.29
HY600	24.4	n.a.	~100	4.56
HY700	24.37	n.a.	~100	4.82

[a] The first four samples are the F_2-treated HY zeolites of the present work. The four last ones are heat-treated HY, Ref. (9). The FAl/Si ratios are calculated from Tables 1 and 3 for the fluorinated samples and from the ^{29}Si NMR spectra for the heated HY.

[b] Averaged over 6 reflections.

[c] Average standard deviation.

[d] Averaged over the same reflections and relative to the blank or to HY heated at 400°C.

the total Al content and the Al^{IV} in the fluorinated samples approximates the *increase* in nonframework species.

In earlier studies on USY, the FAl content was obtained by deconvoluting the ^{29}Si NMR spectra (6). However, the error in the evaluation of the FAl content carried on as suggested above is lower when the FSi/FAl is >10 and when the Al^{IV} line is well resolved. In the starting material and in F20, the high-resolution ^{29}Si MAS NMR spectrum contains the weak line attributable to the Si (1Al) and distinguishable from the Si (0Al) line. In F100, the deconvolution of the two lines is hardly possible. In the F300 sample, the translocation of framework aluminum into Fl-NFAl is almost complete. A superficial examination of XRD patterns indicated that the structure was not qualitatively affected by fluorination, except for the F300C sample. A more detailed analysis has been performed by calculating the unit cell parameter *a* from six *hkl* reflections. The *a* values and the average standard deviations are shown in Table 2. The unit cell dimension decreases significantly as fluorination proceeds. This trend is expected if shorter Si–O bonds replace Al–O bonds or, schematically, if

framework Si–O–Al–O–Si

→ framework Si–O–Si + nonframework Al–O. [1]

It is well documented that the unit cell parameter *a* must be closely related to the lattice composition. For instance, Klinowski *et al.* (13) have suggested for NaY zeolites an empirical equation relating *a* to the framework composition FAl/Si,

$$\text{FAl/Si} = 2(c_1 a - a_0)/(c_2 - c_3 a), \quad [2]$$

where a_0 is the unit cell dimension of a hypothetical Al-free zeolite and where c_1, c_2, and c_3 are arbitrary constants, characteristic of a specified zeolite lattice.

In Fig. 2, the unit cell dimensions *a* measured for our fluorinated samples and for a set of four HY zeolites dealuminated by calcination (with no significant change in crystallinity, Hong *et al.* (9)) are plotted with respect to the measured FAl/Si ratio. For the zeolite dealuminated by dry calcination up to 700°C, FAl/Si was obtained from the deconvolution of the ^{29}Si NMR spectra. For small FAl/Si, as for the fluorinated samples, the plot is apparently linear. For larger FAl/Si Eq. [2] applies, with a_0 = 24.207 Å and

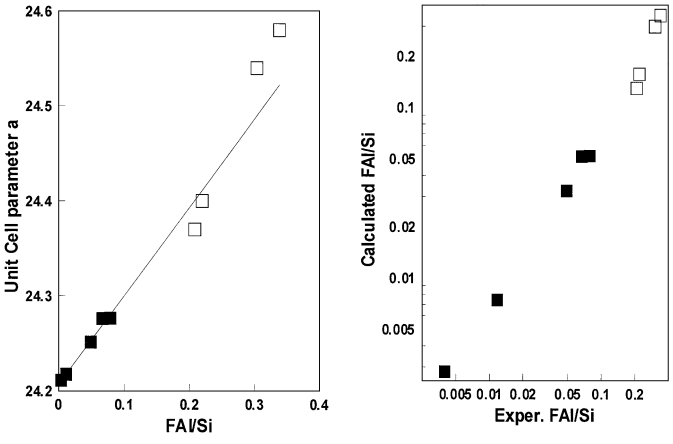

FIG. 2. (A) Variation of the averaged unit cell dimension *a* with respect to the FAl/Si ratio: (■) fluorinated samples, (□) samples dealuminated by calcination, Ref. (9). (B) Calculation of FAl/Si using the empirical equation (2), but with $c_1 = 43.7$, $c_2 = 1.69$, $a_0 = 24.207$ Å, and the experimental *a* values.

$c_3 = 1.69$. In the Klinowski equation, these parameters were 24.05 Å and 1.65, respectively. The differences are probably due to the decationation of the original material, e.g., HY, instead of NaY. From these results, it can be suggested that, after the removal of a fraction of the lattice aluminum, the lattice be cured by the formation of a siloxane bridge in agreement with Eq. [1]. This astonishing healing process will be studied separately as a function of the lattice topography and, in particular, of the number of Al atoms in the first and second coordination shells of silicon. According to Hong *et al.* (9), the nonframework aluminum species remain in the zeolitic pores and decrease the microporous volume accordingly. The crystallinity has been estimated from the sum of the integrated intensities (14, 15) of the diffraction lines used for the calculation of *a*. The sum is referenced to the value obtained likewise for the starting material. The crystallinity does not decrease with dealumination. Instead, a slight increase is observed in agreement with earlier work (6). In F300C, the crystallinity is lost, also in agreement with observations on the thermal dealumination above 800°C.

In F300H, the intensity of the 63 ppm line increases again, as shown in Fig. 3. This suggests either the formation of an alumina spinel or the insertion of a fraction of Al^{VI} (from Fl-NFAl) as Al^{IV} FAl. If a spinel were formed, the $Al^{VI}(O_6)$ resonance would be anomalously upfield since it should be near +10 ppm as in F300C (7). Observe also, in Table 1, the decrease in the F content in the F300H sample compared to that in uncalcined F300.

In F300C, upon calcination and further removal of HF and of water, the nature of the nonframework species is evidently altered, and the Al^{IV} resonance broadens. The overall ^{27}Al NMR spectrum at that stage is typical of an amorphous spinel-like alumina.

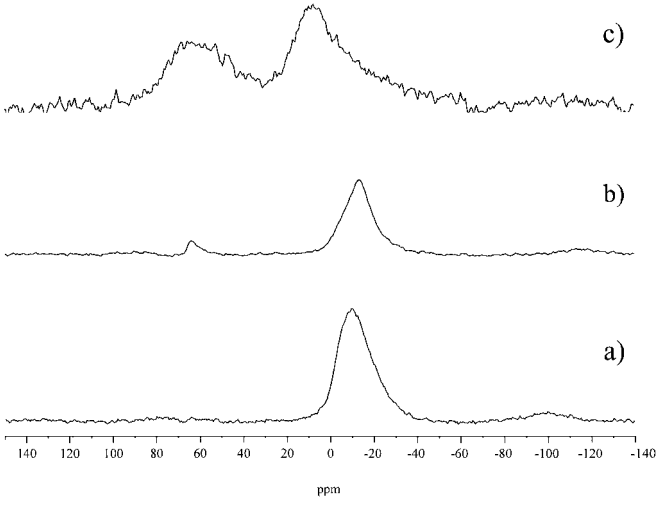

FIG. 3. ^{27}Al NMR spectra of (a) F300, (b) F300H, and (c) F300C samples.

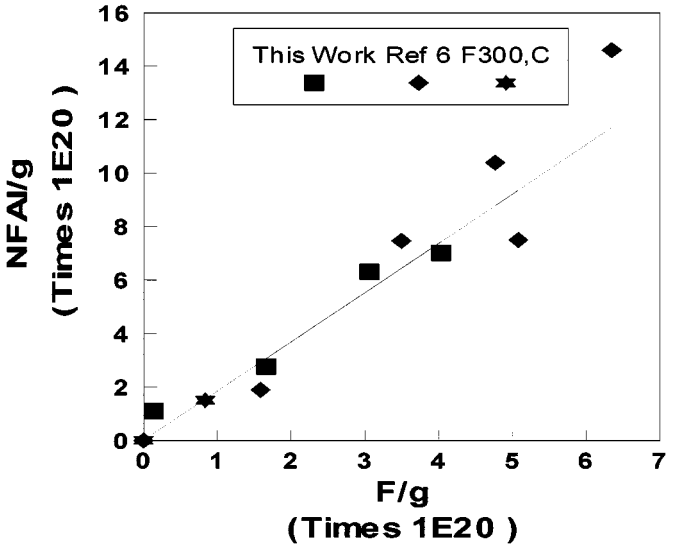

FIG. 4. Linear regression between the nonframework aluminum content, NFAl, and the F content, both in atom-g/g dry zeolite. The NFAl content in F300C is obtained by interpolation.

The NFAl content is proportional to the F content (Fig. 4). The R^2 of the linear regression is 0.963, and the slope is 1.84 NFAl/F or 0.54 F/Al^{VI}. The data obtained by Panov *et al.* (6) have been reanalyzed for comparison with the present findings. Thus, in Fig. 4, the difference between the absolute NFAl content and that of the initial USY obtained from the ^{29}Si NMR spectra is plotted against the F content, see Table 3, Ref. (6). Considering the differences between the experimental procedures (in the ammonium fluoride treatment, the impregnated sample has to be calcined at 500°C in order to incorporate F into the solid) the agreement between the earlier results and those presented here is striking. Thus it seems safe to conclude that, irrespective of the nature of the treatment, the stoichiometry in the Fl-NFAl species is near 0.5 F/Al^{VI}. The higher F contents in USY, compared to HY, are thus attributable to higher Al contents. Indeed, the chemical atomic ratio Si/Al is 2.5 in USY. The eventual back transfer of Al into the lattice at

TABLE 3

Al NMR Analysis

Sample	FAl line int, a.u.	FAl/FAl (init)	FAl/gZ $\times 10^{20}$	NFAl/gZ $\times 10^{20}$
HY	40	1	7.4	0
F20	34	0.85	6.3	1.1
F100	25	0.625	4.6	2.8
F300	2	0.050	0.37	7.0
F300, H	5.8	0.145	1.1	6.3
F300, C	n.m.	n.m.	n.m.	(1.55)[a]

[a] Interpolated from F content and linear regression.

about 500°C suggested in the molecular fluorine treatment had not been observed in the NH_4 treatment.

Thus, in agreement with the XRD data, the silicon–oxygen network keeps its identity. A similar conclusion was previously reached by Lok *et al.* (10) (for HY), Becker and Kowalak (16) and Gosh and Kydd (17) (for mordenite and ZSM-5), and by Panov *et al.* (6) (for USY).

The characterization of the nonframework species is supported also by the FT-IR spectroscopy observations between 540 and 610 cm^{-1}. Figure 5 contains vibrational bands that can be unambiguously assigned to Fl-NFAl, because the HY spectrum is flat in this region (Fig. 5a). The double six-ring band is shifted above 610 cm^{-1} because of the low Al content (18). After fluorination, three bands are observed but they cannot be attributed to specific vibrations. In the AlF_6^{3-} octahedral complex, Nakamoto (19) attributes a band at 541 cm^{-1} to the ν_1 and a band at 568 cm^{-1} to the ν_3 normal modes of vibration of an octahedral molecule respectively. Figure 5b shows how the 570 cm^{-1} band in F300 becomes broader and weaker as the sample is heated at 500°C (F300H) and disappears when the sample is calcined at 1000°C.

Upon heating F300H up to 1000°C, a first signal appears in the TPD trace (Fig. 6) at 100°C due to the removal of physisorbed ammonia, while the relatively weak and broad signal between 300 and 400°C corresponds to the removal of chemisorbed ammonia. In the untreated sample (blank), this signal is much stronger. The decrease of the intensity of the ~400°C signal has to be assigned to the almost complete disappearance of the Brønsted acid sites and to the removal

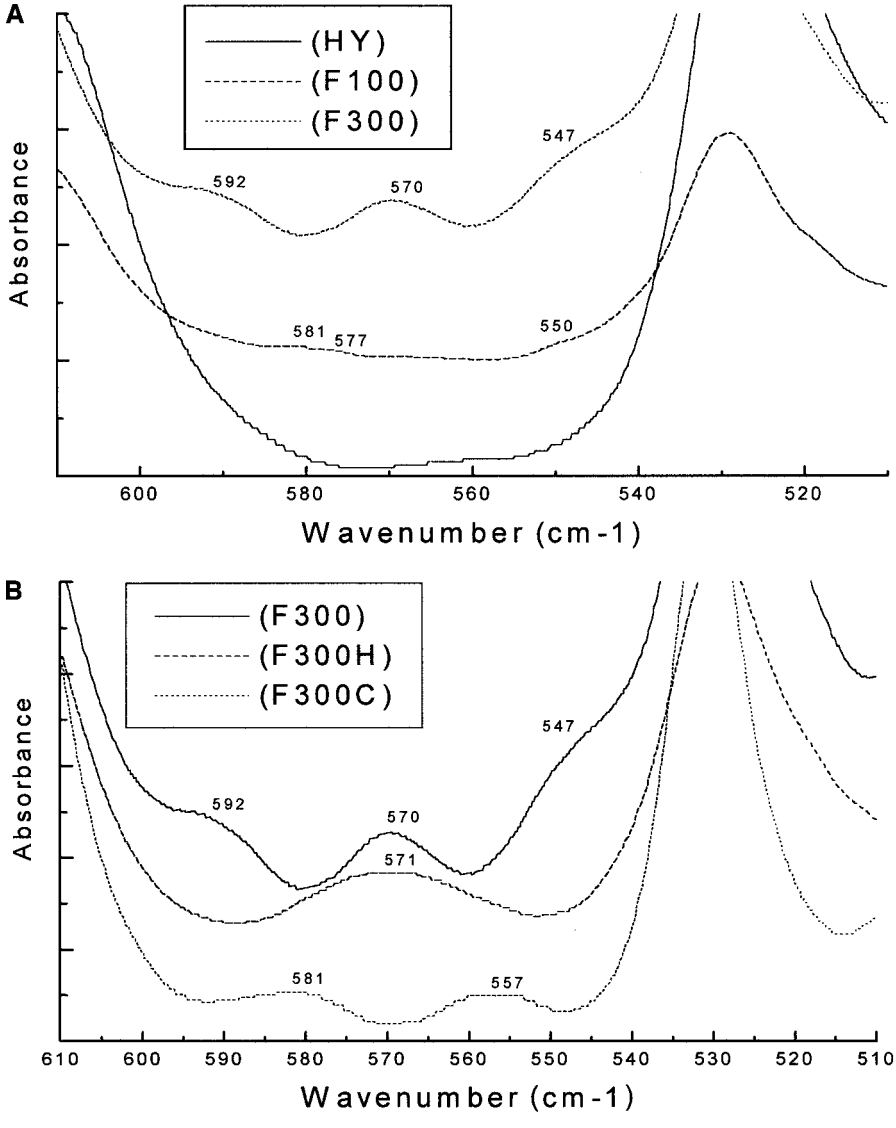

FIG. 5. FT-IR absorbance spectra between 610 and 510 cm^{-1}. The broad bands are most probably those of Fl-NFAl: (A) increasing fluorination, (B) F300, F300H, and F300C.

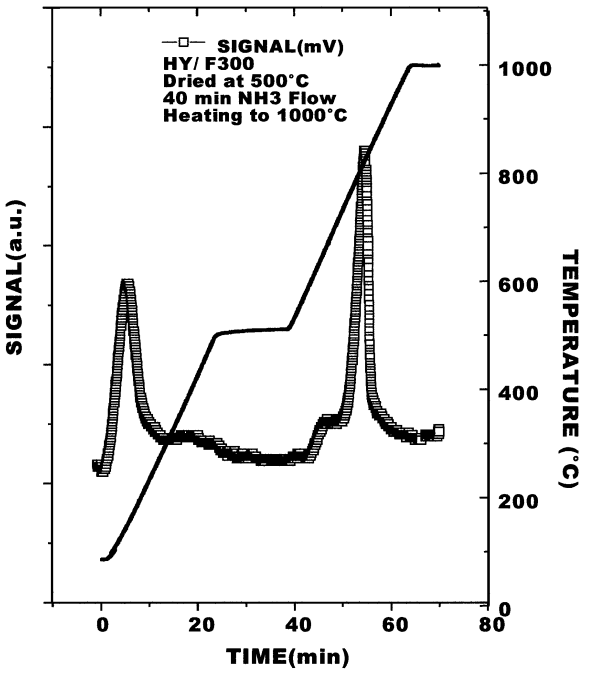

FIG. 6. TPD trace obtained for F300 in a flow of He (30 ml/min) mixed with NH_3 (30 ml/min), as described in the Experimental section.

of the framework aluminum. The high-temperature signal in Fig. 6 is observed at 800°C. It is flanked by a shoulder at ~600°C. Its intensity increases with the fluorine content, indicating that it probably originates from the thermal decomposition of F1-NFAl species. This point was confirmed by TGA which shows a weight loss of ~2% in this interval of temperature.

The thermal decomposition of the Fl-NFAl species at 1000°C results in the formation of HF and of Al_2O_3, the latter species being responsible for the Al^{VI} NMR resonance at about 0 ppm in Fig. 3c. Heating below 600°C would produce aluminum monofluoride monoxide AlFO, H_2O, and HF (20). The monofluoride is a gas at room temperature.

The formation of AlFO is detectable in the FT-IR analysis of the gas phase (Fig. 7). As the solid is heated, a weak band is observed at 1150 cm^{-1} below 600°C that may be assigned to AlO stretching in AlFO. A still weaker band is detectable at 740 cm^{-1}, at the frequency assigned to the Al–F stretch. As the temperature increases from 600 to 1000°C a somewhat stronger band appears at 1027 cm^{-1}. This can be identified with the Si–F stretching frequency in SiF_4 (21).

Around 600°C, the coordination shell of the nonframework fluorinated octahedral species becomes unstable, and Al^{IV} is reincorporated into the zeolite framework. The amount of volatile aluminum or silicon fluoride detected is minute. With respect to the F content in F300, the losses of F in F300H and in F300C amount to 21% and 80%, respectively. Since the Si or Al contents are not significantly affected, it must be concluded that the most probable carrier of fluorine is HF. It has, however, not been detected in the TGA-IR spectra. As it can evolve only from a reaction of fluorine with hydroxyl groups (hydration and coordination water is already outgassed at these temperatures), Fl-NFAl must contain an amount of OH groups comparable to the F content. The existence of a composition such as $Al^{VI}{}_2F(OH)_n(H_2O)_m^{(5-n)+}$ would be compatible with the experimental observations reported above, as well as with the removal of HF upon heating.

The analogy with earlier data by Cowley and Scott (22) is enlightening. A set of structures of general formulas $Al^{VI}F_x(OH)_y \cdot {}_nH_2O$ has been solved by X-ray diffraction. Their structures are cubic ($Fd3m$, $Z = 16$) and $0.7 \leq x \leq 1.96$, $1.04 \leq y \leq 2.3$, and $0 \leq n \leq 3.8$. They dehydrate at about 400°C. The stoichiometry of nonframework species can be expected to be different because of eventual residual links with the lattice (23).

A deeper knowledge of the nature of Fl-NFAl species can be gained through ^{19}F MAS NMR spectroscopy (Fig. 8). The observed chemical shifts, referred to as C_6F_6 or CF_3Cl, are tabulated in Table 4.

The spectra show three types of resonances. First, a small broad contribution appears around −10 ppm: it is of constant absolute intensity regardless of the fluorine content and, therefore, is visible only after the normalization of the intensities in the less fluorinated sample. Such a shift corresponds to a partially hydrated $AlF_3 \cdot nH_2O$ species as observed on fluorinated aluminas (5). This comparison, together with the invariance of this peak position with the fluorine content, suggests that it corresponds to the fluorination of the small amount of extraframework alumina already present in the untreated HY (Fig. 1a).

Second, a set of four sharp resonances without spinning side bands are observed at 7.3 ± 0.2 ppm, 9.1 ± 0.8 ppm,

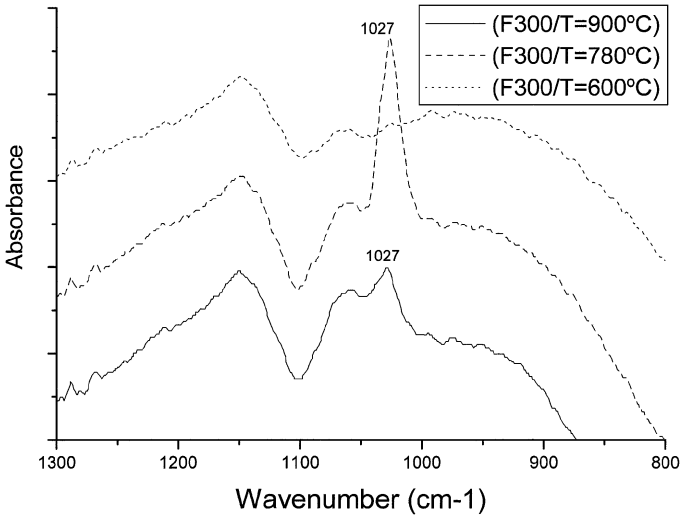

FIG. 7. TGA FT-IR analysis of the volatile removed from the fluorinated zeolite upon heating between 600°C and 1000°C. The amplitude of the largest peak at 1027 cm^{-1} is 0.012 absorbance units.

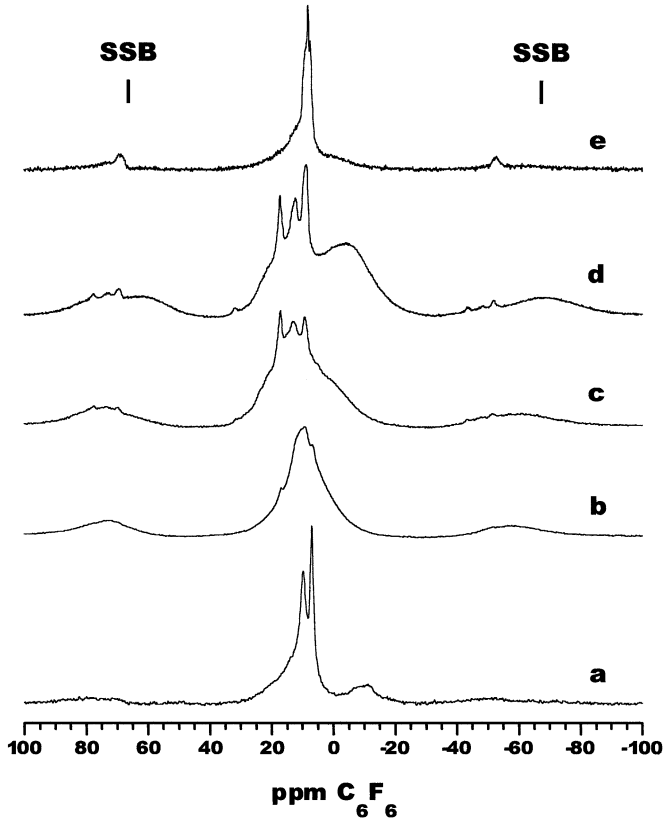

FIG. 8. ^{19}F NMR spectra of (a) F20, (b) F100, and (c) F300 samples. The spectra of F300H and F300C are shown in (d) and (e), respectively. The approximate position of the spinning side bands (SSB) is indicated. Intensities are normalized.

12.8 ± 0.4 ppm, and 17.2 ± 0.1 ppm. Their relative intensities increase, from the most to the least shielded, with increasing fluorine content. Third, there is a broad resonance at about 20 ppm with strong spinning side bands.

A rigorous assignment of these lines to defined species is not possible in the present situation. However, some interesting observations can be made. The lack of spinning side bands is most probably due to an averaging of the chemical shift anisotropy and homonuclear coupling by a high mobility. The presence of mobile F-containing molecular species in all samples constitutes important information. Thus Fl-NFAl is likely composed of ionic species that likely were generated upon the rehydration of the fluorinated zeolite by atmospheric moisture. On the other hand, the broad line suggests the simultaneous presence of less mobile (nonionic) component(s).

TABLE 4

^{19}F NMR Chemical Shifts (*)[a]

Sample	F20	F300, C	F100	F300, H	F300
F cont wt.%	0.044	0.264	0.524	0.966	1.27
Fchem.sh., ppm					
7.3, (−155.7)	*	*			
9.1, (−153.9)	*		*	*	*
12.8, (−150.2)				*	*
17.2, (−145.8)				*	*
≅−10 ppm, broad (≅−173)	*		*	*	*
20 to −10, broad (−144 to −173)	*		*	*	*

[a] Values between parentheses are referred to CF_3Cl.

The chemical shift of the resonances of the mobile species in our samples can be compared with those obtained for complexes in solution. Sur and Bryant (24) have studied fluoroaluminum complexes in solution and adsorbed by zeolite. They have assigned sharp lines from 7 to 11 ppm to complexes such as $AlF_x^{(3-x)+}$, as found in other studies on aqueous solutions (25, 26). The more positive the complex, the more upfield is the shift. By analogy (Table 4), the line at 7.3 ppm should correspond to the most positive complex while the line at 17.2 ppm would be due to the most negative species. However, since here the ratio F/Al seems constant, a variation of the charge implies that the number of OH^- in the complexes is variable. The ^{19}F shift would become more positive as this number increases. The "neutral" complex in the work by Sur and Bryant (24) has a shift of 8.6 ppm, with respect to C_6F_6, close to that of the ubiquitous line at *ca.* 9 ppm observed in all our samples. The additional lines around 7 ppm at low F content and around 13 ppm and 17 ppm at higher F contents would account for complexes such as $(Al_2{}^{VI}F(OH)_n \cdot H_2O_m)^{(5-n)+}$, with lower or higher OH contents. The OH contents would thus be quite variable in the Fl-NFAl species, while the F/Al^{VI} ratio would be quite constant. It is also worthwhile to note that no line attributable to free F^- has been observed at −44.5 ppm (27).

As for the nonmobile species with strong spinning side bands, a valid comparison with fluorinated aluminas can be carried on. D'Espinose *et al.* (5) observed broad but resolved lines at −10, 9, 20, and 33 ppm that they assigned to partially hydrated AlF_3 and to $(Al^{VI}O_5F)$, $(Al^{VI}O_4F_2)$, and $(Al^{VI}O_3F_3)$ environments on the alumina surface, respectively. This chemical shift range is therefore compatible with the present observation. Decanio *et al.* (28) observed shifts at −10 ppm or at −20 ppm in fully hydrated or dehydrated AlF_3, respectively. The lack of resolution could reflect the higher degree of disorder expected in highly dispersed Fl-NFAl compared to a fluorinated γ-Al_2O_3, as well as higher homonuclear coupling due to the high F content in Fl-NFAl.

POSSIBLE REACTION MECHANISM

The products of the reaction of molecular fluorine with poorly hydrated HY having been reasonably identified, a possible reaction mechanism will be sketched. Table 5

TABLE 5

Bond Strengths of Diatomic Molecules[a]

SiO	799.6 kJ/mol
AlF	663.3 kJ/mol
HF	569.87 kJ/mol
SiF	552.7 kJ/mol
AlO	511.0 kJ/mol

[a] Source: "CRC Handbook of Chemistry and Physics," 51st Ed. CRC Press, Boca Raton, 1999.

illustrates the thermodynamic justification of what follows. It shows bond strengths in diatomic molecules.

It seems probable that the first step is the reaction of F_2 with the acid center and the formation of HF and of a nonframework fluorinated species weakly attached to the lattice (**A**).

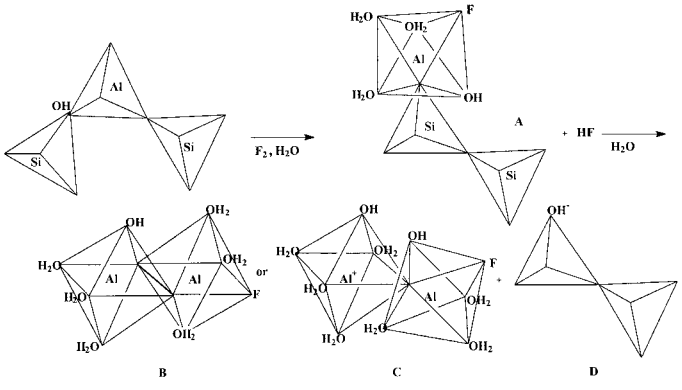

Upon hydrolysis by atmospheric moisture, this surface species would become mobile and dimerization would become possible. Hydration and dimerization could yield a neutral complex such as **B** or an ionic complex such as **C** with OH^- counteranions. **D** is the residual silica backbone of the dealuminated zeolite with eventual silanol terminations.

The residual water content of HY pretreated in the reactor at 200°C would not be larger than 1 wt%, rendering the initial step possible. Indeed, after contact with the atmosphere, there would be plenty of water to activate dimerization and the formation of ionic complexes.

Heating at 500–600°C would depolymerize and produce volatile AlFO and HF. A small fraction of the aluminum would be available for insertion into the lattice but the major part would form a disordered spinel phase in the zeolite micropores. One may argue about the aluminum reinsertion. In Fig. 3b, the weak line at 63 ppm might not be very convincing. The fact that the FAl/Si ratio calculated along this hypothesis fits into the function relating *a* and FAl/Si; Fig. 2a is an additional argument. Moreover, insertion of aluminum from $(NH_4)_3AlF_6$ solution into dealuminated ZSM-5 and silicalite has been reported previously (29).

At higher temperatures fluorine could eventually react with silicon through the surface silanol groups.

CONCLUSIONS

The first conclusion reached from the ^{27}Al NMR study is that fluorination of HY by molecular gaseous F_2 at room temperature results in an extensive dealumination of the framework. It is a fast reaction that comes to completion within about 10 min at room temperature. The average composition of the reaction product is one F for two nonframework Al (Fig. 4). This ratio is identical to what has been observed in a USY zeolite systems fluorinated by impregnation with ammonium fluoride at 500°C.

In HY the structural element likely to be attacked first is the Si–OH–Al bridge. Aluminum is removed quantitatively from the framework by fluorine, and the essential part of the fluorine is located on the NFAl species. Becker and Kowalak (16) had already observed a quantitative relationship between the extent of fluorination and the initial Al contents in mordenite and ZSM-5.

A second striking bit of information is the conservation of the silicate backbone despite the translocation of aluminum from its position in the lattice to nonframework fluorinated species. Conversely, the vacancies left by aluminum are filled probably by the formation of a siloxane bridge between two silanols, in silicon tetrahedra, which were separated by a FAl tetrahedron and which become adjacent.

A third point uncovered by ^{19}F NMR in this study is that, besides fluorinated alumina, Al oxy-hydroxy-fluoride(s) ionic octahedral complexes of the type $Al_2F(OH)_n^{(5-n)+}$ are produced. These complexes undergo (reversible) dehydration above 500°C, resulting perhaps in a partial reincorporation of aluminum in the zeolite framework. They are finally destroyed above 800°C, that is, at a temperature at which SiF_4 degasses.

Thus, the room-temperature solid-state transformation studied here offers the challenging opportunity to prepare, in one step, a well-crystallized microporous silica in which molecular size species are dispersed.

REFERENCES

1. Startsev, A. N., Klimov, O. V, Kalinkin, A. V., and Mastikhin, V. M., *Kinet. Catal.* **35**, 552 (1994).
2. Gosh, A. K., and Kydd, R. A., *Catal. Rev.-Sci. Eng.* **27**, 539 (1985).
3. Fischer, L., Thesis, Université de Paris VI, 1999.
4. Saniger, J. M., Sanchez, N. A., and Flores, J. O., *J. Fluorine Chem.* **88**, 117 (1998).
5. Fisher, L., Harle, H., Kasztelan, H. S., Man, P. P., and d'Espinose de la Caillerie, J. B., *Solid State Nucl. Magn. Reson.* **16**, 85 (2000).

6. Panov, A. G., Gruver, V., and Fripiat, J. J., *J. Catal.* **168**, 321 (1997).
7. Coster, D., Blumenfeld, A. L., and Fripiat, J. J., *J. Phys. Chem.* **98**, 6201 (1994); Blumenfeld, A. L., Coster, D., and Fripiat, J. J., *J. Phys. Chem.* **99**, 15181 (1995).
8. Gruver, V., and Fripiat, J. J., *J. Phys. Chem.* **98**, 8549 (1994).
9. Hong, Y., and Fripiat, J. J., *Microporous Mesoporous Mater.* **4**, 323 (1995).
10. Lok, B. M., Gorstema, F. P., Messina, C. A., Rastelli, H., and Izod, T. P., *ACS Symp. Ser.* **218**, 41 (1983).
11. We thank Quim. Rufino Lozano of the Insituto de Geología, for X-ray fluorescence analyses and M. en C. Leticia Baños of the Instituto de Materiales of the Universidad Nacional Autónoma de México for X-ray diffraction.
12. Bodkin, J. B., *Analyst* **102**, 409–413 (1976).
13. Klinowski, J., Thomas, J. M., Fyfe, C. A., and Gobbi, G. C., *J. Chem. Soc., Faraday Trans. 1* **81**, 3003 (1985).
14. ASTM standards, D 3942-91,15.03 (1991), 612.
15. ASTM standards, D3906-91,15.03 (1991), 597.
16. Becker, K. A, and Kowalak, S. J., *in* "Recent Advances in Zeolite Science" (J. Klinowski and P. J. Barie, Eds.), p. 123. Elsevier, New York, 1989.
17. Ghosh, A. K., and Kydd, R. A., *J. Catal.* **103**, 399 (1987).
18. Flanigen, E. M., Khatami, H., and Szymansky, H. A., "Molecular Sieve Zeolites 1," Adv. Chem. Series 101, pp. 201–229. Am. Chem. Soc., Washington, DC, 1971.
19. Nakamoto, K., "Infrared and Raman Spectra of Inorganic and Coordination Compounds," 4th Ed. Wiley, New York, 1986.
20. NIST, Standard Reference Data Program, CAS Registry Number 13596-12-8.
21. NIST, Standard Reference Data Program, CAS Registry Number 7783-61-1.
22. "Crystal data, Determinative Tables," 2nd Ed. (J. H. Donnay, G. Donnay, E. G. Cox, O. Kennard, and M. V. King, Eds.), pp. 954 and 955 data by Cowley and Scott. Am. Crystallographic Assoc., New York, 1963.
23. Alvarez, L. J, Ramirez Solis, A., and Bosch Giral, P., *Zeolites* **18**, 54 (1997).
24. Sur, S. K., and Bryant, R. G., *Zeolites* **16**, 118 (1996).
25. Martinez, E. J., Girardet, J. L., and Morat, C., *Inorg. Chem.* **35**, 706 (1996).
26. Hansen, E. W., Vistad, Ø. B., Akporiaye, D. E., Lillerud, K. P., and Wendelbo, R., *J. Phys. Chem. A* **103**, 2532 (1999).
27. Patarin, J., Caulet, P., Marler, B., Faust, A. C., and Guth, J. L., *Zeolites* **14**, 675 (1994).
28. Decanio, E. C., Bruno, J. W., Nero, V. P., and Edwards, J. C., *J. Catal.* **140**, 84 (1993).
29. Dessau, R. M., and Kerr, G. T., *Zeolites* **4**, 315 (1984).